ACS OMEGA

Open Access

http://pubs.acs.org/journal/acsodf

Article

Rhenium−Pyrazolyl-Based Figure-Eight- and Z-Shaped Metallocycles: Self-Assembly, Solid-State Structures, Dynamic Properties in Solution, and Competitive Ligand-Induced Supramolecular Transformations into Rhenium-Pyridyl/-Benzimidazolyl/-Phosphine-Based Metallocycles/Acyclic Complexes

Upasana Phukon, Moon Kedia, Bhaskaran Shankar, and Malaichamy Sathiyendiran*

Cite This: *ACS Omega* 2023, 8, 41773−41784

Read Online

ACCESS | Metrics & More | Article Recommendations | Supporting Information

ABSTRACT: Rhenium(I)tricarbonyl core-based heteroleptic "figure-eight"- and Z-shaped metallocycles (**1a**−**4a**) of the general formula *fac*-[{$(CO)_3Re(\mu$-L)$Re(CO)_3\}_2(dppz)_2$] were self-assembled from $Re_2(CO)_{10}$, H_2-L (H_2-L = 5,8-dihydroxy-1,4-naphthaquinone (H_2-dhnq) for **1a**; 1,4-dihydroxy-9,10-anthraquinone (H_2-dhaq) for **2a**; 6,11-dihydroxy-5,12-naphthacenedione (H_2-dhnd) for **3a**; 2,2′-bisbenzimidazole (H_2-bbim) for **4a**), and bis(4-((pyrazolyl)methyl)phenylmethane) (dppz) via one-pot coordination-driven synthetic approach. The molecular structures of **1a** and **4a** were unambiguously confirmed by single-crystal X-ray diffraction (SC-XRD) methods. The metallocycles in the DMSO solution exist as an acyclic dinuclear−DMSO adduct of the general formula *fac*-[{$(CO)_3Re(\mu$-L)$Re(CO)_3\}(DMSO)_2$] (**1b**, L = dhnq; **2b**, L = dhaq; **3b**, L = dhnd; **4b**, L = bbim) and dppz, which are in dynamic equilibrium. The dynamic behavior of the rhenium−pyrazolyl bond in the solution state was effectively utilized to transform metallocycles **1a**−**4a** into pyridyl/benzimidazolyl/phosphine donor-based heteroleptic metallocycles and acyclic dinuclear complexes (**4**−**13**). These include tetranuclear rectangles *fac*-[{$(CO)_3Re(\mu$-L)$Re(CO)_3\}_2(4,4'$-bpy)$_2$] (**4** and **11**, L = dhaq for **4** and bbim for **11**), dinuclear metallocycles *fac*-[{$(CO)_3Re(\mu$-L)$Re(CO)_3\}$(dpbim)] (**5**−**7** and **12**; L = dhnq for **5**, dhaq for **6**, dhnd for **7**, and bbim for **12**), and dinuclear acyclic complexes *fac*-[{$(CO)_3Re(\mu$-L)$Re(CO)_3\}(PTA)_2$] (**8**−**10** and **13**; L = dhnq for **8**, dhaq for **9**, dhnd for **10**, and bbim for **13**). These transformations were achieved through component-induced supramolecular reactions while treating with competitive ligands 4,4′-bipyridine (4,4′-bpy), bis(4-((1*H*-benzoimidazole-1-yl)methyl)phenyl)methane (dpbim), and 1,3,5-triaza-7-phosphaadamantane (PTA). The reaction mixture in the solution was analyzed using NMR and electrospray ionization mass spectrometry (ESI-MS) analysis. Additionally, crystal structures of **4**, **6**, and **13**, which were obtained in the mixture of the solutions, were determined, providing unequivocal evidence for the occurrence of supramolecular transformation within the system. The results reveal that the size of the chelating ligand and the pyrazolyl donor angle of the ditopic ligand play crucial roles in determining the resulting solid-state metallacyclic architecture in these synthetic combinations. The dynamic behavior of the rhenium−pyrazolyl bond in the metallocycles can be utilized to transform into other metallocycles and acyclic complexes using suitable competing ligands via ligand-induced supramolecular transformations.

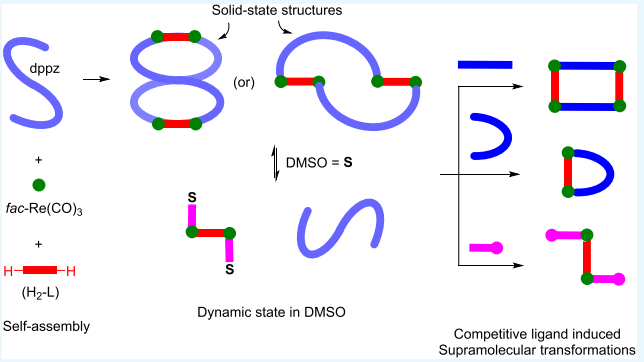

INTRODUCTION

The design and synthesis of metallocycles such as cages, helicates, and simple-to-complex topological architectures via coordination-driven self-assembly have been gaining significant attention owing to their potential applications in materials and medicinal fields.[1−9] Further, new aesthetically appealing molecular architectures including intricate topological metallocyclic architectures such as metallo-links (a series of interlocked metallocyclic rings where at least one ring has to be broken to separate them) and metallo-knots similar to those found in nature can be prepared using the self-assembly.[10−18] Among various topologies, "figure-eight" architecture is one of the elegant self-assembled structures, which is found in natural systems such as Lissoclinamide 7, the recombinant structure of

Received: August 26, 2023
Revised: September 23, 2023
Accepted: October 10, 2023
Published: October 30, 2023

Scheme 1. Self-Assembly of Metallocycles 1a−4a

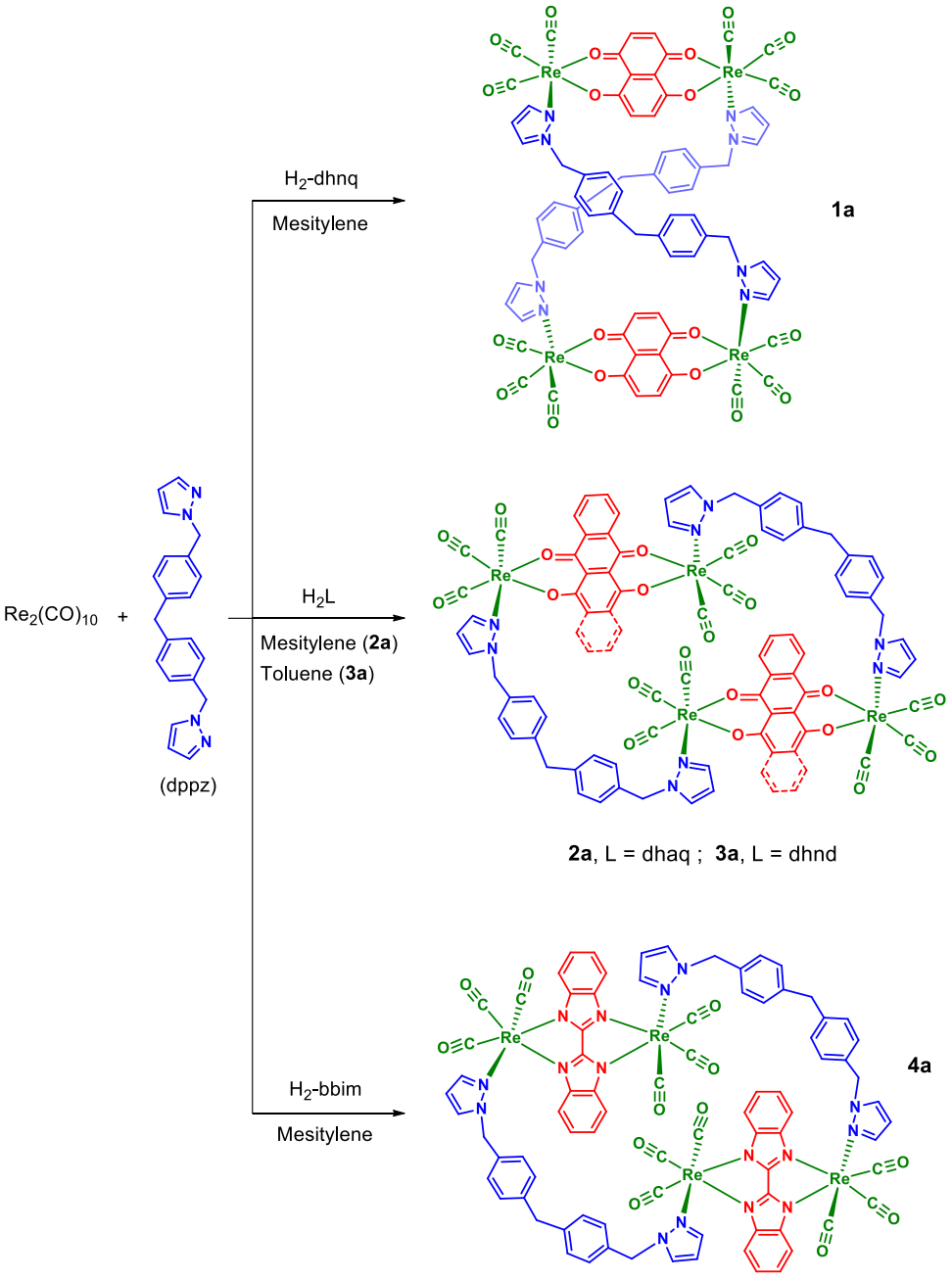

circular DNA and marine alkaloid.[19,20] However, very few examples of "figure-eight"-shaped metallocycles are known until now.[21−26] The design and synthesis of "figure-eight"-shaped metallocycles and other metallocyclic architectures using various metal precursors and organic building units are important in the development of the field, which might yield molecules having various potential applications in the near future. Among the few metal ion-based coordination-driven approaches, the *fac*-[Re(CO)$_3$] core-based self-assembly method is one of the methods to construct neutral homoleptic and heteroleptic metallocycles, which have potential applications in the field of host−guest encapsulation, catalysis, selective reactivity, sensing, and as bioactive agents.[27−57] Although a considerable number of synthetic principles for the preparation of various sizes and shapes of *fac*-[Re(CO)$_3$] core-based metallocycles are currently available, synthetic approaches for preparing "figure-eight" topology, complex-knot, and complex-link-shaped metallocycles are scarce. In addition to the metal core, the nature of the ligand is crucial to obtaining complex topological architectures. To the best of our knowledge, pyridyl and imidazolyl/benzimidazolyl and their structural analogous-based ditopic/tritopic and multitopic ligands are frequently used to construct *fac*-[Re(CO)$_3$] core-based metallocycles. These rhenium(I)-based metallocycles are generally kinetically inert and robust in solution, including the coordinating DMSO solvent. On the other hand, only a countable number of pyrazolyl donor-based ligands are used in constructing *fac*-[Re(CO)$_3$] metallocycles[46,58] It is well-known that metal−pyrazolyl bonds are labile in the donor solvents. It is expected that the rhenium−pyrazolyl bond in the metallocycles can also be dynamic in the donor solvent. This dynamic nature of metal−donor bonds in the metallocycles can be

https://doi.org/10.1021/acsomega.3c06371
ACS Omega 2023, 8, 41773−41784

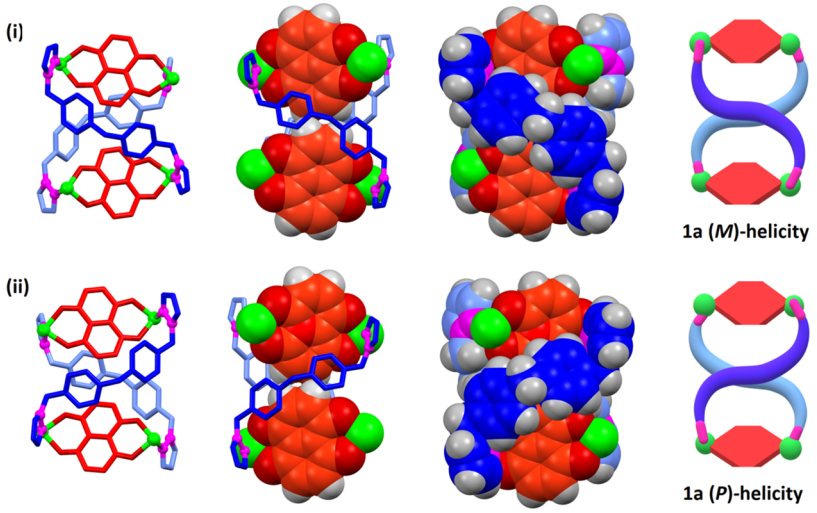

Figure 1. Various views of "figure-eight"-shaped metallocycle **1a** showing both (*M*)-helicity and (*P*)-helicity. Carbonyl groups are removed for clarity. Color code: Re = green; red = $dhnq^{2-}$; blue/pale blue with pink = dppz with N; and H = gray.

utilized potentially both in supramolecular transformations and as an active agent for biological systems. However, the design, synthesis, and structural transformation of a rhenium−pyrazolyl motif containing metallocycles are unknown.

We have used the flexible ditopic pyrazolyl donor (dppz) consisting of biphenylmethane (−CH_2−Ph−CH_2−Ph−CH_2−) as a spacer and utilized it in constructing a new type of helicate with the bis-chelating ligand and $Re_2(CO)_{10}$.[46] In this approach, both the rigid ligand (H-L) and the coordination angle of pyrazolyl donor play an important role in dictating the helical structure because the flexible ditopic ligand containing the same spacer with the benzimidazolyl donor yields metallocavitand.[47] Therefore, we envision that modulating the width and the length of the rigid bis-chelating ligands (H-L) in the self-assembly combinations of $Re_2(CO)_{10}$, H-L, and dppz would result in hitherto unknown metallocycles including "figure-eight" architecture, metallo-links, or metallo-knots. Hence, rigid bis-chelating ligands 5,8-dihydroxy-1,4-naphthaquinone (H_2-dhnq), 1,4-dihydroxy-9,10-anthraquinone (H_2-dhaq), 6,11-dihydroxy-5,12-naphthacenedione (H_2-dhnd), and 2,2′-bisbenzimidazole (H_2-bbim) having different widths and lengths were chosen along with dppz in the present study. These rigid bis-chelating ligands are widely used in the construction of supramolecular coordination complexes including Ir/Rh-based metallo-links/metallo-knots and a considerable number of Re molecular rectangles, which have potential applications in the medicinal and material field.[16,56,57]

Herein, we combine the self-assembly of pyrazolyl motif-based *fac*-[$Re(CO)_3$] core metallocycles, study their dynamic behavior in DMSO solution, and utilize the dynamic nature of the rhenium−pyrazolyl bond in creating potential new metallocycles and acyclic complexes via ligand-induced supramolecular transformation. In this paper, we report on a neutral heteroleptic "figure-of-eight"- and "Z"-shaped metallocycles (**1a**−**4a**), which were self-assembled using $Re_2(CO)_{10}$, rigid bis-chelating ligands, and dppz in a one-pot approach. The solid-state structures of **1a** and **4a** were determined by single-crystal X-ray diffraction analysis. The metallocycles are in dynamic equilibrium with disassembled dinuclear−DMSO complexes (**1b**−**4b**) and dppz in the solution state. The dynamic nature of the Re-pyrazolyl bond of the metallocycles was fruitfully utilized further to transform these metallocycles into other nitrogen donor-based tetranuclear and dinuclear metallocycles and phosphine donor-based dinuclear acyclic complexes (**4**−**13**) via ligand-exchange process, which were studied using NMR, ESI-MS analysis, and single-crystal X-ray analysis.

RESULTS AND DISCUSSION

Synthesis and Characterization of 1a−4a. Compounds **1a**−**4a** were synthesized by treating $Re_2(CO)_{10}$, rigid bis-chelating ligand (H_2−dhnq for **1a**; H_2−dhaq for **2a**), and dppz in mesitylene under a one-pot reflux approach (Scheme 1). Compounds **3a**−**4a** were synthesized by treating $Re_2(CO)_{10}$, rigid bis-chelating ligand (H_2−dhnd for **3a**; H_2−bbim for **4a**), and dppz in toluene for **3a** and in mesitylene:hexane for **4a** under a one-pot solvothermal approach (Scheme 1). The products are stable in air and moisture. All of the complexes displayed two strong C≡O stretching bands in the region of 2017−1872 cm^{-1} (2010 and 1882 cm^{-1} for **1a**; 2008 and 1886 cm^{-1} for **2a**; 2011 and 1872 cm^{-1} for **3a**; 2017 and 1882 cm^{-1} for **4a**), characteristic of *fac*-[$Re(CO)_3$] motif in an asymmetric environment (Figures S1, S3, S10, and S17 in the SI). The formation of tetranuclear structures in solution was further confirmed by ESI-mass analysis, which shows molecular ion peaks (*m*/*z*: 2115.1687 for [**1a** + H]$^+$; 2215.1185 for [**2a** + H]$^+$; *m*/*z*: 2315.1704 for [**3a** + H]$^+$; *m*/*z*: 2203.2252 for [**4a** + H]$^+$) that matches with the theoretical values (Figure 5, S7−S9, S14−S16, and S21−S23 in the SI).

Molecular Structures of Metallocycles 1a and 4a. The molecular structures of **1a** and **4a** were confirmed by single-crystal X-ray diffraction analysis. Both complexes adopt a M_4L_2L'-type supramolecular metallocyclic structure and consist of four *fac*-[$Re(CO)_3$] cores, two dianionic bis-chelating dhnq/bbim motifs, and two dppz ligands (Figure 1). The asymmetric unit of complex **1a** consists of one metallocycle and five mesitylene solvent molecules. The overall shape of complex **1a** can be best described as a "figure-eight" topology. This can be viewed as the dinuclear *fac*-[{$Re(CO)_3$}(dhnq){$Re(CO)_3$}] motif as one node and the dppz motif as an "S"-shaped helical framework unit. Two dppz motifs helically coordinated to two dinuclear nodes resulting in the "figure-eight" metallomacrocyclic architecture.

https://doi.org/10.1021/acsomega.3c06371
ACS Omega 2023, 8, 41773−41784

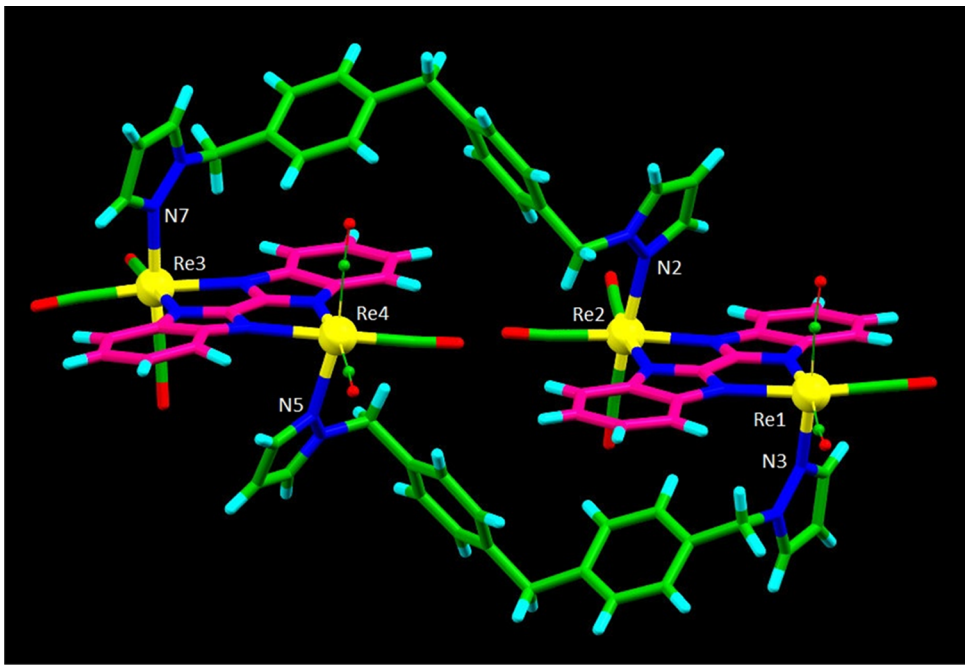

Figure 2. Molecular structure of metallocycle **4a**. Four carbonyl groups are shown as a thin ball-and-stick model for clarity. Color code: C = green/purple, N = blue, O = red, and H = aqua.

The unit cell of **1a** contains two metallocycles and ten mesitylene solvent molecules. One metallocycle adopts (*M*)-helicity (50%), whereas the other metallocycle adopts (*P*)-helicity (50%). The two dhnq units in **1a** are positioned one over the other where the edge of the one dhnq faces the edge of the another dhnq (dihedral angle = ∼31°), i.e., no face-to-face stacking of the two dhnq units. The closest H···H contacts between two dhnq units are 2.348 and 2.652 Å, indicating weak noncovalent dispersion contacts present between these units. The two dhnq units almost act as one central twisted rigid strand, restricting any direct intramolecular noncovalent contacts between the aromatic units of the two dppz motifs. However, intramolecular noncovalent contacts are present between the dhnq motif and the phenyl unit of the dppz motif. The dppz ligand adopts a *syn-anti* cofacial arrangement, i.e., two phenyl units are V-shaped and two pyrazolyl units are arranged *anti*-cofacially. The N···N distance of dppz in **1a** is 12.16/12.33 Å (N1···N5/N7···N3). The pyrazolyl unit is coordinated to the rhenium core and is *trans* to the carbonyl unit. The plane of the pyrazolyl ring is not overlying on the plane of the dhnq unit. The biphenyl spacer is arranged as a V shape with the dihedral angle of 117/111°. Among the biphenyl units, the one adjacent to the coordinated pyrazolyl unit overlie the dhnq unit in a face-tilted manner.

The molecular structure of **4a** consists of four *fac*-[$Re(CO)_3$] cores, two bis-benzimidazolate motifs, and two dppz motifs (Figure 2). The complex adopts "Z"-shaped tetranuclear metallocyclic architecture. The overall sizes of the metallocycle are 22.4 Å (length, terminal ···O along the Re···Re axis), 13.5 Å width, and 11.2 Å (height, length of bbim). The rhenium core is surrounded by three carbonyl groups that are arranged in a facial manner, one chelating motif from bbim, and one pyrazolyl motif. Rhenium(I) adopts an octahedral geometry. Among the four rhenium tricarbonyl groups, two are arranged by directing their carbonyl groups outward and another two *fac*−$Re(CO)_3$ are arranged at the center by directing two of their carbonyl groups inward. The dianionic bbim ligand bischelates two Re cores symmetrically with Re···Re distances of 5.71 Å (Re1···Re2) and 5.72 Å (Re3···Re4). The bond distances of the two-chelating ring and the C−C distance (which connects two bim units) are 1.42(3) and 1.43(3) Å, revealing that the electronic delocalization of the π-system occurs in the bridging site, i.e., imidazolate unit. The Re−N bond distance is 2.21−2.23 Å, which is well within the expected range.[46,58,61] Two $bbim^{2-}$ units are arranged side by side, i.e., almost in the same plane. The dppz ligand adopts a *syn-anti*-cofacial arrangement, i.e., two phenyl units are V-shaped and two pyrazolyl units are arranged *anti*-cofacially. The N···N distances of dppz in **4a** are 12.550, 12.665 and 12.616, 12.479 Å (N3···N5/N7···N2). The pyrazolyl unit is coordinated with the rhenium *trans* to the carbonyl unit and is oriented along the Re−CO axis. The plane of the pyrazolyl ring is not overlying on the plane of the bbim unit. The biphenyl spacer is arranged as a V shape with a dihedral angle of 97/91°. Among the two phenyl units, one adjacent to the coordinated pyrazolyl unit overlies the bbim unit in a face-tilted manner. The two pyrazolyl units of the bidentate ligand are coordinated to two rhenium atoms, each coordinated with one bis-chelating motif. This type of arrangement leads to a metallocycle of a longer length. The crystal structure of **4a** showed various types of intermolecular interactions including weak H-bonding interactions (H···O ≡ C−Re) that play a profound role in the supramolecular network structure.[60] Along the "*c*"-axis, molecules are packed in "*abab*" pattern, forming a supramolecular helical superstructure via C−H···π (C20−H···C45 = 2.959 Å and 175°) and C−H···O ≡ C−Re (C21−H···O2 = 2.505 Å and 145°). Three adjacent molecules along the *c*-axis interact noncovalently, resulting in a one-dimensional helical twist with a distance of 59 Å. Along the *b*-axis, a columnar pattern was found, and intermolecular C−H···O ≡ C−Re (C59−H···O12 = 2.65 Å and 151°; C54−H···O5 = 2.658 Å and 148°) and Re−C ≡ O(5)···O(10) ≡ C−Re (2.916 Å and 109°/98°) contacts hold the two adjacent molecules.

https://doi.org/10.1021/acsomega.3c06371
ACS Omega 2023, 8, 41773−41784

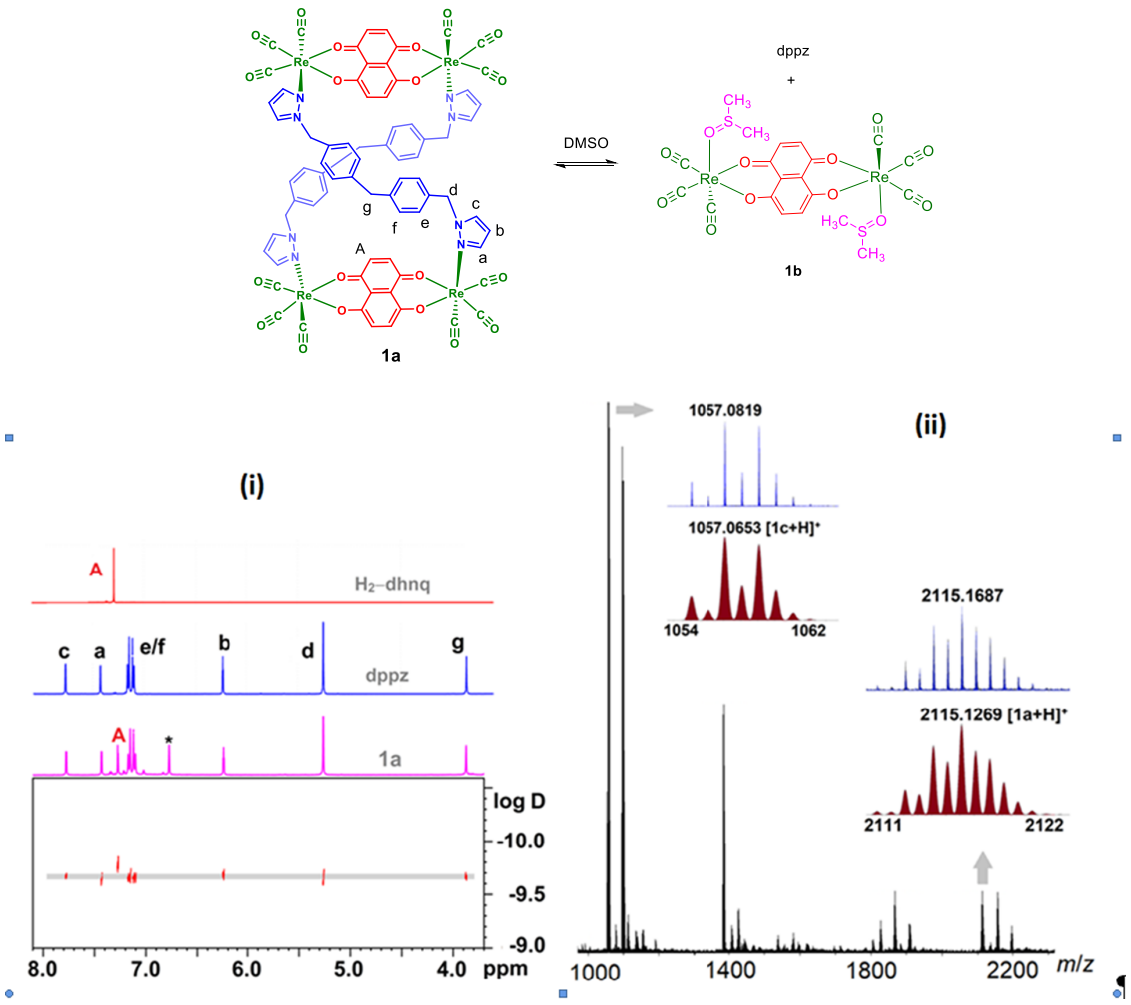

Figure 3. (i) ^{1}H NMR spectra of H_2-dhnq and dppz and the ^{1}H DOSY spectrum of disassembly products of **1a** in d_6-DMSO. (ii) HR-ESI-MS spectrum of **1a** inset shows experimental and calculated isotopic distribution for peaks corresponding to "figure-eight" tetranuclear $[\mathbf{1a} + H]^+$ and dinuclear $[\mathbf{1c} + H]^+$ in a solvent.

Solution Dynamics and Structural Transformation. It is well-known that metal-*N*(pyrazolate/pyrazolyl/pyrazole)-based complexes undergo various structural transformations in the solution due to the dynamic nature of the metal−pyrazolyl bond.[24,58,59,61−63] The solid-state structures of pyrazolyl-based complexes may differ in the solution state. Therefore, the stability of the metallocycles and the exact nature of the coordination motifs present in the solution state are worth studying due to the fact that the *fac*-$[Re(CO)_3]$ core-based acyclic complexes and metallocycles have potential applications in the biomedical fields.[28−30] Metallocycles **1a−3a** are sparingly soluble in $CHCl_3$, acetone, and DMSO at room temperature and completely soluble in hot DMSO, whereas complex **4a** is soluble only in hot DMSO. All of the complexes were dissolved in hot d_6-DMSO, allowed to cool down to room temperature, and used for further studies. No precipitate was observed from the d_6-DMSO solution of the metallocycles during the studies and even after a period of two to three days. The ^{1}H NMR spectra of **1a−4a** in d_6-DMSO displayed well-separated peaks for both the bis-chelating ligand and dppz motifs (Figures 3 and S2, S4−S6, S11−S13, and S18−S20 in the SI).

In all of the cases, the protons of the bis-chelating ligand were slightly/significantly downfield/upfield shifted relative to the free bis-chelating ligands, suggesting the coordination of the ligand to the metal cores. A doublet peak corresponding to the H^A protons of the $dhnq^{2-}$ motif (δ = 7.26 ppm, J = 2.5 Hz) was observed in **1a** and was upfield shifted as compared to that of the proton of free dhnq. The protons of dhaq appeared as two multiplets (H^{B-C}) and one unsymmetrical doublet (H^A) with a coupling constant of 2.0 Hz in **2a**. Among these peaks, H^B was shifted downfield, whereas H^C and H^A were shifted upfield relative to that of free H_2-dhaq, suggesting the coordination of the $dhaq^{2-}$ motif in **2a**. The protons (H^A and H^B) of dhnd in **3a** appeared as two well-separated multiplets with equal intensity. The H^A peak was shifted slightly downfield compared to that of the free H_2-dhnd. The proton (H^{A-B}) signals of bbim in **4a** appeared as two multiplets and were downfield shifted relative to that of free H_2-bbim. The data indicate that the bis-chelating ligand symmetrically coordinated to two rhenium cores.

On the other hand, the signals of the protons of the dppz in **1a−4a** remain similar to that of the free dppz. It is well-known that the proton adjacent to the coordinated nitrogen atom generally shifts to the downfield region due to the loss of electron density. Further, the C−H proton directing toward the π-electron cloud undergoes an upfield shift due to the ring current effect. Based on the X-ray structures, the protons of the

https://doi.org/10.1021/acsomega.3c06371
ACS Omega 2023, 8, 41773−41784

Scheme 2. Proposed Dynamic Nature of 1a, (or) 2a, (or) 3a and Component-Induced Supramolecular Transformations into Tetranuclear Rectangle (4), Dinuclear Metallocycles (5−7), and Dinuclear Acyclic Complexes (8−10) in DMSO

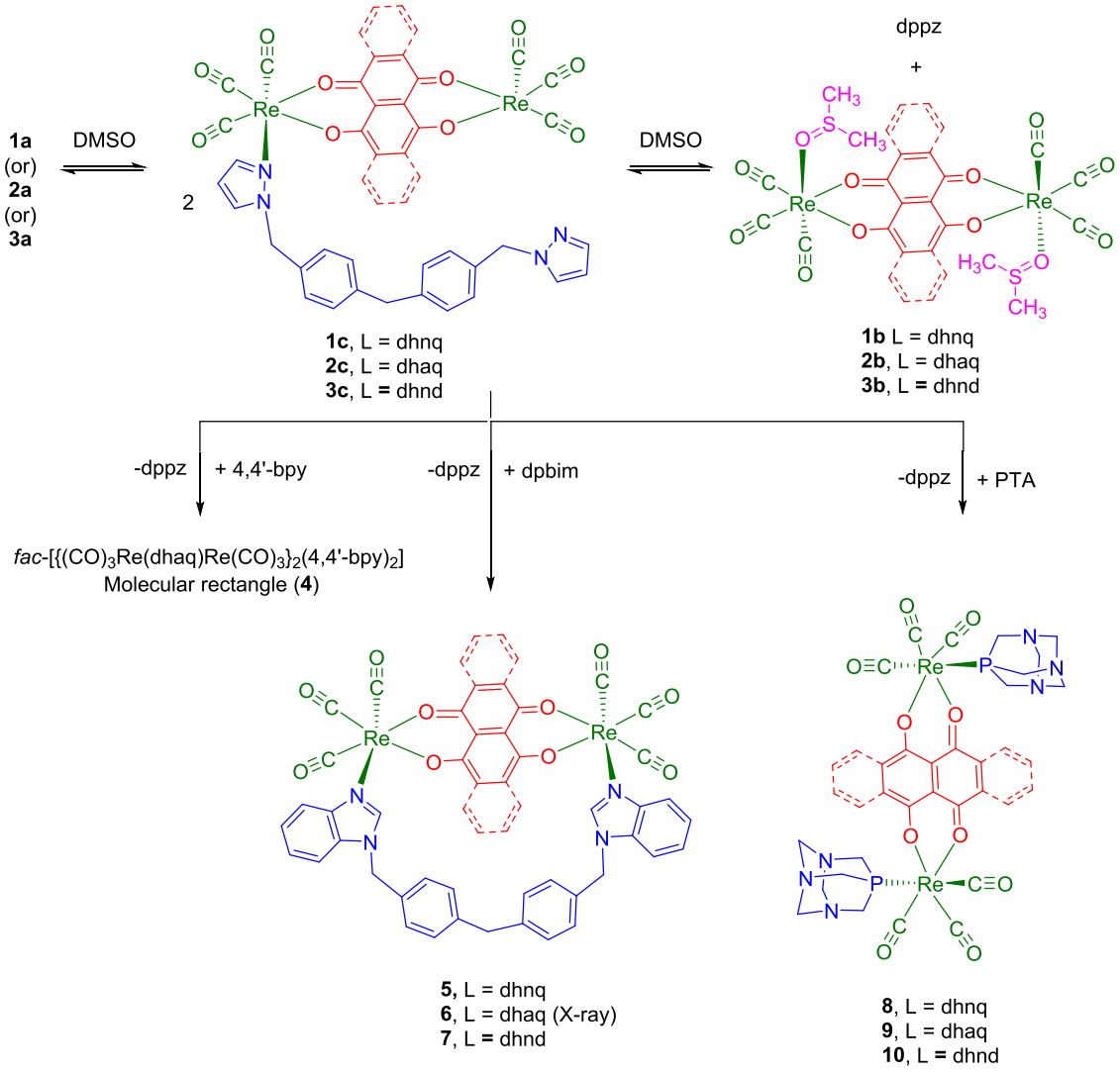

dppz motif are expected to appear in the downfield and upfield regions. However, the protons of dppz did not show any shift in comparison to the free dppz. Therefore, this can be explained if metallocycles **1a−4a** in d_6-DMSO after heating disassembled into acyclic dinuclear−DMSO adduct of the general formula *fac*-[{$(CO)_3$Re(μ-L)Re$(CO)_3$}$(DMSO)_2$] (**1b**, L = dhnq; **2b**, L = dhaq; **3b**, L = dhnd; **4b**, L = bbim) and dppz, which are in dynamic equilibrium (Schemes 2 and3). The disassembled reaction process may proceed via the dinuclear acyclic complexes *fac*-[{$(CO)_3$Re(μ-L)Re$(CO)_3$}-(L)] (**1c**, L = dhnq; **2c**, L = dhaq; **3c**, L = dhnd; **4c**, L = bbim). This is probably because of the labile nature of metal−pyrazolyl bonds observed in many systems and the nonlabile nature of the bis-chelating dinuclear complex.[24,31] Further to attain stable electronic configuration around the rhenium metal center, each metal can receive one DMSO molecule. To understand further the species present in the solution, 2D diffusion-ordered ^{1}H DOSY NMR spectroscopy was carried out. Metallocycle **1a** displays two sets of peaks, which are very close to each other, indicating the presence of two units possibly **1c** and dppz. The ^{1}H DOSY spectra of other metallocycles **2a−4a** showed two types of peaks that are well-separated, suggesting the presence of two motifs in the solution. The value of a one set of the peaks corresponding to the protons of the dppz in all of the complexes is similar to that of the value found for the free dppz. The above result suggested that one of the diassembly products is free dppz, and the other should be the dinuclear−DMSO adduct complexes **1c−4c**. To gain insight into the structure of the molecular species, the solutions were analyzed by ESI-mass spectrometry. All of the metallocycles displayed relatively less intense peaks corresponding to tetranuclear motifs and strong peaks corresponding to the dinuclear complexes (**1c−4c**) (m/z: 1057.0819 for $[\mathbf{1c} + H]^+$; 1107.0808 for $[\mathbf{2c} + H]^+$; m/z: 1157.0852 for $[\mathbf{3c} + H]^+$; m/z: 1101.1126 for $[\mathbf{4c} + H]^+$). The experimental isotopic distribution peaks for both the tetranuclear metallocycles and dinuclear complexes match the theoretical values. No peaks corresponding to the DMSO adduct of dinuclear complexes **1b−4b** were found in the ESI-MS spectra. The ^{1}H NMR and ESI-MS analysis of **1a−4a** in DMSO solution indicates the dynamic nature of the metallocycles.

Component-induced supramolecular transformations in metallocycles occur because of rearrangement or partial or

https://doi.org/10.1021/acsomega.3c06371
ACS Omega 2023, 8, 41773−41784

Scheme 3. Proposed Dynamic Nature of 4a and Component-Induced Supramolecular Transformations into Tetranuclear Rectangle (11), Dinuclear Metallocycle (12), and Dinuclear Acyclic Complex (13) in DMSO

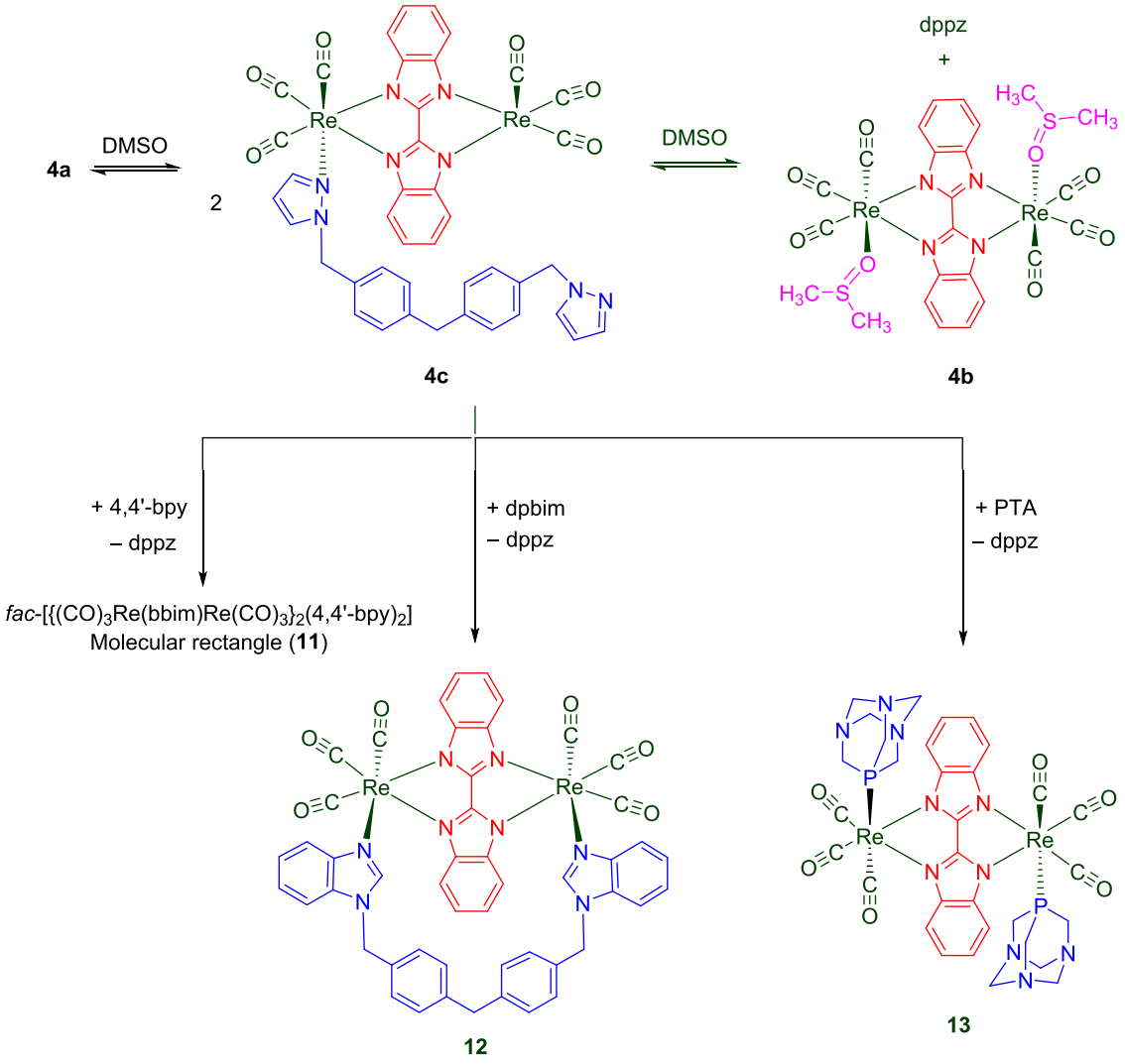

complete disassembly of the structural framework units upon the addition of another competitive building block, which leads to the formation of more stable or new discrete supramolecular structures.[64−68] To utilize the dynamic nature of M−N (rhenium−pyrazolyl) bond and the dynamic nature of metallocycles **1a−4a** in the DMSO solution (Schemes 2 and3), competitive selectivity studies were carried out using different donor ligands such as 4,4′-bipyridine (4,4′-bpy), 4,7-phenanthroline (4,7-Phen), bis(4-((1*H*-benzoimidazole-1-yl)-methyl)phenyl)methane (dpbim) (dpbim), and 1,3,5-triaza-7-phosphaadamantane (PTA). The supramolecular reactions of the metallocycles with the chosen ligands were carried out by adding an equivalent or excess amount of the donor to the DMSO-d_6 solution of the metallocycles, followed by heating, analyzing using ^{1}H NMR and ESI-mass analysis.

When 4,4′-bpy was subjected to a DMSO-d_6 solution of **1a−4a**, changes were observed in the ^{1}H NMR spectra for complexes **2a** and **4a**, particularly the appearance of new proton peaks that correspond to coordination of 4,4′-bpy to the rhenium core as found in **4** and **11** (Figures S24, S29, S34, and S41 in the SI).[56,57] This indicates that structural transformation takes place by a ligand-exchange process. Supramolecular structural transformation occurring in the present case was further confirmed by X-ray analysis of single crystals formed in the NMR tube containing **4a** and 4,4′-bpy in DMSO-d_6. The solid-state structure unambiguously confirmed the formation of molecular rectangle *fac*-[{Re-$(CO)_3$}$_4$(bbim)$_2$(4,4′-bpy)$_2$] (**11**).

However, tetranuclear heteroleptic molecular rectangles consisting of *fac*-[Re$(CO)_3$] cores, two bbim^{2-}, and two 4,4′-bpy units are known.[56] Hence, no detailed discussion of the molecular structure of molecular rectangle **11** is included. Surprisingly, no proton peak shifts of 4,4′-bpy were observed in the ^{1}H NMR spectrum of **1a** + 4,4′-bpy and **3a** + 4,4′-bpy in DMSO-d_6, indicating that ligand exchange did not occur in these cases.

The ligand 4,7-Phen is rarely used in the construction of *fac*-[Re$(CO)_3$] core-based metallocycles. The known 4,7-Phen-based rhenium metallocycles contain either a dhnq or dhaq motif.[35] Therefore, supramolecular transformation reactions of metallocycles **1a−4a** with 4,7-Phen were attempted. Upon the addition of 4,7-Phen to the DMSO-d_6 solution of **1a−4a**, no changes were observed in the ^{1}H NMR spectra of the complexes (Figures S25, S30, S35, and S42 in the SI). The ESI-mass spectra of the above mixture did not show any peaks corresponding to the expected new and known tetranuclear

https://doi.org/10.1021/acsomega.3c06371
ACS Omega 2023, 8, 41773−41784

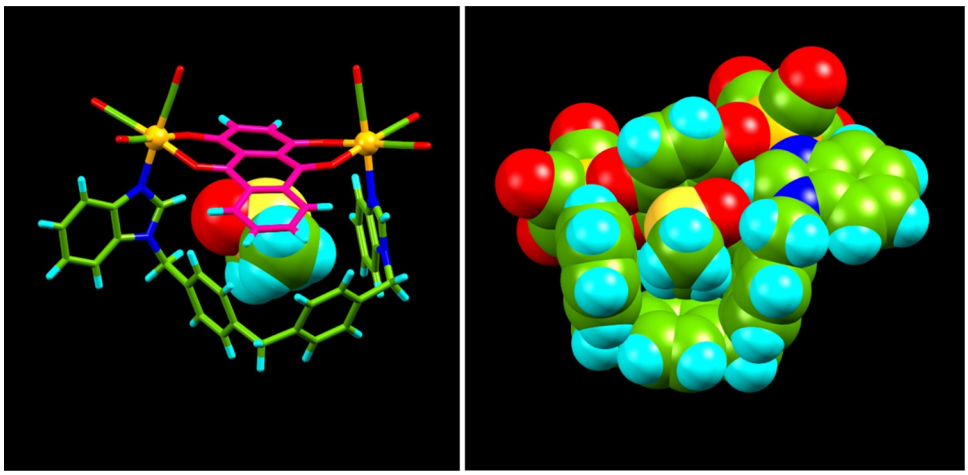

Figure 4. Stick (back view) and space-filling (front view) representations of metallocycle **6** with a DMSO guest molecule. Color code: C = green/purple, H = aqua, N = blue, O = red, S = yellow, and Re = orange.

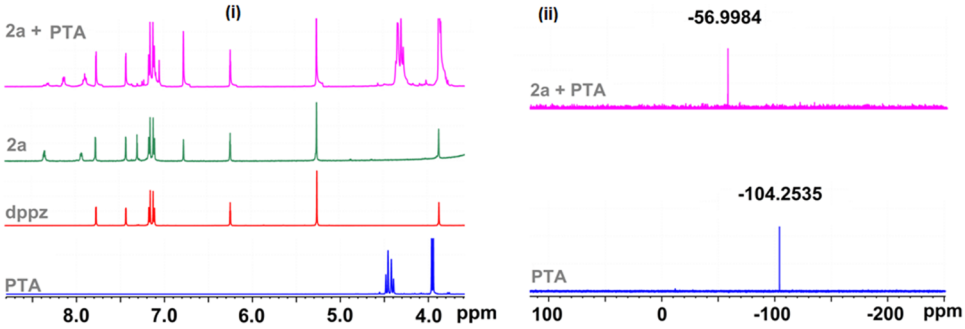

Figure 5. (i) Partial ^{1}H NMR spectra of PTA, dppz, **2a**, and **2a** + PTA in d_6-DMSO. (ii) ^{31}P NMR spectra of PTA and **2a** + PTA in d_6-DMSO (**2a** = powder **2a** was dissolved in d_6-DMSO).

metallocycles. The data indicate that dppz is the preferred ligand over 4,7-Phen in the current self-assembly combinations.

Further, when a competitive experiment was performed with a benzimidazolyl-based ditopic donor dpbim in the solution of complexes **1a**−**4a**, the ^{1}H NMR spectra showed the binding of the dpbim ligand over the dppz ligand with the appearance of new sets of peaks, which were shifted relative to the free dpbim ligand (Figures S26, S31, S36, and S43 in the SI). The ESI-mass spectra of the mixture displayed molecular ion peaks (m/z: 1259.1300 for $[7 + H]^+$ and 1203.1549 for $[\mathbf{12} + H]^+$), confirming the formation of dinuclear complexes *fac*-[{Re$(CO)_3$}$_2$(L)(dpbim)] (where L = dhnd for **7**; bbim for **12**) (Figures S37, S38, S44 and S45 in the SI). Our group previously reported the formation of dinuclear metallocycle by the reaction of H_2-dhnd/H_2-dhaq, $Re_2(CO)_{10}$, and dpbim. Among the metallocycles, the complexes comprising dhnd were unambiguously proven by SC-XRD analysis. The ligand-exchange phenomenon was further confirmed by the solid-state structure of **6**, which adopts a dinuclear M_2LL'-type metallocyclic structure (Figure 4).

The rhenium tricarbonyl cores are chelated by rigid dianionic bis-chelating dhaq and clipped by a neutral dpbim nitrogen donor. The dhaq motif is significantly above the Re··· Re plane and bent toward the center of the metallocycle. The distance between two Re atoms is found to be 8.41 Å, and the N2···N3 distance is 9.16 Å. The benzimidazolyl motifs of the dpbim ligand are arranged with a dihedral angle of 76°. The orientations of both the ligand frames create an internal cavity, which perfectly accommodates solvent DMSO. The DMSO molecule is stabilized in the cavity via cumulative hydrogen bonding (d = C21−H···O═S$(CH_3)_2$ = 2.25 Å, 141°; d = C49−H···O═S$(CH_3)_2$ = 2.43 Å, 127°) contacts and CH···π interactions, which occurs between the methyl units of DMSO and π surface of both the benzimidazolyl motif and dhaq unit. The guest molecule dictates the unusual arrangement of the metallocycle, which is facilitated by the flexible nature of the neutral ditopic ligand. One molecule of **6** interacts with an adjacent molecule via Re−C≡O(6)···O(19) ≡C−Re (2.97 Å), Re−C≡O(5)···O(18)≡C−Re (2.92 Å) interactions to form a noncovalent dimer. This dimer further interacts with another adjacent dimer via CH···π contacts between the benzimidazolyl motif of one and the phenyl spacer unit of another.

Similarly, 1,3,5-triaza-7-phosphaadamantane (PTA) was added to the d_6-DMSO solution of complexes **1a**−**4a**. Changes in both the ^{1}H and ^{31}P NMR spectra were observed, indicating that the ligand exchange takes place with PTA, resulting in acyclic dinuclear complexes *fac*-[{Re$(CO)_3$(TPA)}$_2$(L)] (where L = dhnq for **8**; dhaq for **9**; dhnd for **10**; bbim for **13**) (Figures 5 and S27, S28, S39, S40, S46 and S47 in the SI). Among these complexes, complexes **9** and **10** exist as a single isomer in the solution, which is based on the appearance of a single peak (δ = −56.99 ppm for **9** and δ = −56.56 ppm for **10**) in ^{31}P NMR, which are downfield shifted relative to the free PTA ligand (δ = −104.25 ppm) (Figure 5).

On the other hand, the ^{31}P NMR spectrum of complex **10** displayed four peaks (δ = −11.978, − 57.2397, − 77.6733, and −85.4257 ppm) with different intensities, which are downfield

https://doi.org/10.1021/acsomega.3c06371
ACS Omega 2023, 8, 41773−41784

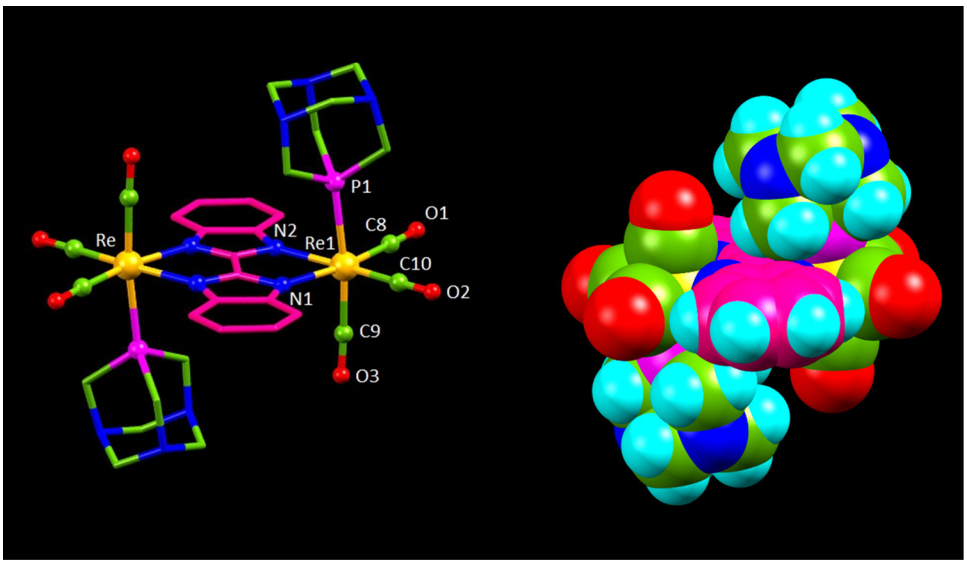

Figure 6. Ball-and-stick and space-filling representations of the molecular structure of **13**. Color code: C = green/purple, H = aqua, N = blue, O = red, S = yellow, and Re = orange.

shifted compared to those of free PTA ligand possibly because of the presence of isomers in the solution. The ^{31}P NMR spectrum of complex **13** displayed four peaks (δ = −71.21, −71.43, − 72.44, and −72.69 ppm) with different intensities, which are significantly downfield shifted compared to those of the free PTA ligand. The data proves that the phosphorus ligand coordinated with the rhenium center. The ESI-MS spectra of the mixture of metalloocycle and PTA displayed peaks (m/z = 1092.1028 for $[\mathbf{9} + H]^+$, m/z = 1087.1148 for $[\mathbf{13} + H]^+$), corresponding to the acyclic dinuclear complexes (Figures S32, S33, S48 and S49 in the SI).

Further, the formation of complex **13** was also confirmed by SC-XRD analysis. Single crystals suitable for XRD data collection were obtained from the NMR tube after a week. The molecular structure of **13** shows that it is a dinuclear acyclic complex having two *fac*-$Re(CO)_3$ cores, one dianionic bbim motif, and two PTA ligands (Figure 6). The geometry around the rhenium centers is distorted octahedral with a C_3O_2P donor environment. The bbim ligand is almost planar and coordinated with two rhenium cores symmetrically. The PTA ligand is coordinated with a rhenium center using its phosphorus atom. The two PTA ligands in the complex are arranged in a "Z-type" *trans*-position. The Re−C distances *trans* to the *N,N*(bbim) atoms are 1.922 Å (Re1−C8) and 1.914 Å (Re1−C10), whereas the Re−C distance trans to the P(PTA) atom is 1.931 Å (Re1−C9). The longer Re−C distance *trans* to PTA can be ascribed to the *trans* effect of PTA due to the stronger π-acceptor ability of PTA.[69−71] The Re···Re distance is 5.753 Å, which is in the expected range. Each molecule interacts with the neighboring molecule through various intermolecular and supramolecular interactions. Two neighboring molecules are arranged in such a way that the PTA of one molecule faces the PTA of another molecule, which contact each other through C−H···N hydrogen bonding interactions (d = C15−H···N8 = 2.705 Å; C14−H···N8 = 2.672 Å) and C−H···H−C dispersion contacts (d = C13−H···H−C14 = 2.340 Å).

CONCLUSIONS

In conclusion, neutral heteroleptic metallocycles having "figure-of-eight"-shaped architecture and a "Z′-type" structure (**1a−4a**) were obtained from $Re_2(CO)_{10}$, rigid bis-chelating ligands, and flexible ditopic pyrazolyl donor dppz. To the best of our knowledge, this is the first synthetic report on heteroleptic *fac*-$[Re(CO)_3]$ core-based coordination-driven self-assembly approach for figure-of-eight-shaped metallocycle. The metallocycles were found to be in dynamic equilibrium with disassembly products in the solution state. The dynamic nature of the rhenium−pyrazolyl coordination bond in the metallocycles was further utilized in transforming the metallocycles into pyridyl/benzimidazolyl nitrogen donor-based metallocycles such as molecular rectangles (**4**, **11**), dinuclear metallocycles (**5−7**, and **12**), and phosphine donor-based acyclic complexes (**8−10** and **13**) via component-induced supramolecular transformation reactions with the addition of various types of competing ligands. The results reveal that modulation of the size of the rigid bis-chelating ligand and the coordination angle of pyrazolyl donor directs the final shape of the metallocyclic architecture during the self-assembly process, thereby providing insights for design of hitherto unknown *fac*-$[Re(CO)_3]$ core-based intricate topological architectures including figure-eight supramolecules. Further, rhenium metallocycle coordinated with the pyrazolyl ligand is attractive because of the easily breakable rhenium−pyrazolyl bond in a DMSO solution. The pyridyl/imidazolyl ligands have the ability to substitute the pyrazolyl donors through supramolecular transformation. The results may pave the way to the development of less explored competitive ligand-induced supramolecular transformations in rhenium carbonyl-based metallocycles.

MATERIALS AND METHODS

$Re_2(CO)_{10}$, pyrazole (H−pz), diphenylmethane, H_2-dhnq, H_2-dhaq, H_2-dhnd, KOH, DMF, HBr-acetic acid (33%), paraformaldehyde, *o*-phenylenediamine, hexachloroacetone, orthophosphoric acid, NBS, CCl_4, toluene, mesitylene, hexane, and ethylene glycol were purchased and used as received. H_2-bbim and dppz were prepared by following known

https://doi.org/10.1021/acsomega.3c06371
ACS Omega 2023, 8, 41773−41784

procedures.[47] ATR-IR spectra were recorded on a Nicolet iS5 IR spectrophotometer. NMR spectra were recorded on a Bruker Avance III 500 MHz spectrometer. High-resolution ESI-MS (HR-ESI-MS) spectra were recorded on a Bruker-maXis mass spectrometer. Single-crystal X-ray data of **1a**, **4a**, **6**, and **13** were collected on a Rigaku Oxford Diffractometer ($\lambda_{(Mo\ K\alpha)}$ = 0.71073 Å). The molecular structures were solved by direct methods using SHELXS-97 (Sheldrick 2008) and refined using the SHELXL-2018/3 program (within the WinGX program package).[72,73] Non-H atoms were refined anisotropically.

Synthesis of *fac*-[{(CO)$_3$Re(μ-dhnq)Re(CO)$_3$}$_2$(dppz)$_2$] (1a). A mixture of $Re_2(CO)_{10}$ (50.0 mg, 0.076 mmol), H_2-dhnq (14.6 mg, 0.076 mmol), dppz (25.1 mg, 0.076 mmol), and mesitylene (20 mL) was refluxed for 5 h and cooled to 30 °C. A dark green precipitate obtained was filtered, washed with hexane, and air-dried. Yield: 35% (115 mg). Green crystals suitable for single-crystal X-ray diffraction analysis were obtained from the filtrate. The ^{1}H NMR spectra of precipitate and crystals are the same. AT-IR (cm^{-1}): 2010 (s) and 1882 (s) (C ≡ O). HR-ESI-MS (*m*/*z*): [M + H]$^+$ calcd for $C_{74}H_{49}N_8O_{20}Re_4$, 2115.1269; found, 2115.1687. ^{1}H NMR (500 MHz, DMSO−d_6, ppm): 7.76 (d, *J* = 1.5 Hz, 4H, H^c), 7.42 (d, *J* = 1.5 Hz, 4H, H^a), 7.26 (d, *J* = 2.5 Hz, 4H, H^A), 7.16 (d, *J* = 5 Hz, 8H, H$^{e/f}$), 7.11 (d, *J* = 5 Hz, 8H, H$^{e/f}$), 6.24 (t, *J* = 1 Hz, 4H, H^b), 5.25 (s, 8H, H^d), 3.86 (s, 4H, H^g).

Synthesis of *fac*-[{(CO)$_3$Re(μ-dhaq)Re(CO)$_3$}$_2$(dppz)$_2$] (2a). A mixture of $Re_2(CO)_{10}$ (200.0 mg, 0.3065 mmol), H_2-dhaq (74.0 mg, 0.3065 mmol), dppz (101.6 mg, 0.3065 mmol), and mesitylene (30 mL) was refluxed for 5 h and cooled to 30 °C. Compound **2a** was obtained as a dark green powder. The product was filtered, washed with hexane, and air-dried. Yield: 41% (150 mg). AT-IR (cm^{-1}): 2008 (s) and 1886 (s) (C ≡ O). HRMS-ESI (*m*/*z*): [M + H]$^+$ calcd for $C_{82}H_{53}N_8O_{20}Re_4$, 2215.1583; found, 2215.1185. ^{1}H NMR (500 MHz, d_6-DMSO, δ): 8.36−8.43 (m, 8H, H^C), 7.94−7.92 (m, 8H, H^B), 7.76 (d, *J* = 1.5 Hz, 4H, H^c), 7.42 (d, *J* = 1.5 Hz, 4H, H^a), 7.29 (d, *J* = 4 Hz, H^A), 7.16 (d, *J* = 5 Hz, 8H, H$^{e/f}$), 7.11 (d, *J* = 5 Hz, 8H, H$^{e/f}$), 6.24 (t, *J* = 1 Hz, 4H, H^b), 5.25 (s, 8H, H^d), 3.86 (s, 4H, H^g).

Synthesis of *fac*-[{(CO)$_3$Re(μ-dhnd)Re(CO)$_3$}$_2$(dppz)$_2$] (3a). A mixture of $Re_2(CO)_{10}$ (100.1 mg, 0.1532 mmol), H_2-dhnd (45.2 mg, 0.153 mmol), dppz (50.4 mg, 0.153 mmol), and toluene (10 mL) was kept in an oven maintained at 160 °C for 48 h and cooled to 30 °C. Compound **3a** was obtained as a dark purple powder. The product was filtered, washed with hexane, and air-dried. Yield: 27% (48 mg). AT-IR (cm^{-1}): 2011 (s) and 1872 (s) (C ≡ O). HRMS-ESI (*m*/*z*): [M + H]$^+$ calcd for $C_{90}H_{57}N_8O_{20}Re_4$, 2315.1898; found, 2315.1704. ^{1}H NMR (500 MHz, DMSO−d_6, ppm): 8.42−8.39 (m, 8H, H^A), 7.94−7.92 (m, 8H, H^B), 7.76 (d, *J* = 1.5 Hz, 4H, H^c), 7.42 (d, *J* = 1.5 Hz, 4H, H^a), 7.16 (d, *J* = 5 Hz, 8H, H$^{e/f}$), 7.11 (d, *J* = 5 Hz, 8H, H$^{e/f}$), 6.24 (t, *J* = 1 Hz, 4H, H^b), 5.25 (s, 8H, H^d), 3.86 (s, 4H, H^g).

Synthesis of *fac*-[{(CO)$_3$Re(μ-bbim)Re(CO)$_3$}$_2$(dppz)$_2$] (4a). A mixture of $Re_2(CO)_{10}$ (100 mg, 0.153 mmol), H_2-bbim (36.0 mg, 0.156 mmol), dppz (50.5 mg, 0.157 mmol), and mesitylene:hexane (10:2 mL) in a Teflon flask was placed in a steel bomb. The bomb was kept in an oven maintained at 175 °C for 72 h and cooled to 30 °C. Compound **4a** was obtained as light yellow crystals. The product was filtered, washed with hexane, and air-dried. Yield: 50% (84 mg crystals). ATR−IR (cm^{-1}): 2017 (s) and 1882 (s) (C ≡ O). HRMS−ESI (*m*/*z*): [M + H]$^+$ calcd for $C_{82}H_{57}N_{16}O_{12}Re_4$, 2203.2548; found, 2203.2252. ^{1}H NMR (500 MHz, DMSO−d_6, ppm): 7.76 (d, *J* = 1.5 Hz, 4H, H^c), 7.65−7.61 (m, 8H, H^A), 7.42 (d, *J* = 1.5 Hz, 4H, H^a), 7.39−7.37 (m, 8H, H^B), 7.16 (d, *J* = 5 Hz, 8H, H$^{e/f}$), 7.11 (d, *J* = 5 Hz, 8H, H$^{e/f}$), 6.24 (t, *J* = 1 Hz, 4H, H^b), 5.25 (s, 8H, H^d), 3.86 (s, 4H, H^g).

■ ASSOCIATED CONTENT

Supporting Information

The Supporting Information is available free of charge at https://pubs.acs.org/doi/10.1021/acsomega.3c06371.

Characterization spectra (IR, NMR, ESI-MS) of the complexes (PDF)

Compound **1a** (CIF)

Compound **4a** (CIF)

Compound **6** (CIF)

Compound **13** (CIF)

■ AUTHOR INFORMATION

Corresponding Author

Malaichamy Sathiyendiran − *School of Chemistry, University of Hyderabad, Hyderabad 500 046, India;* orcid.org/0000-0002-6699-4998; Email: mvdiran@yahoo.com, msathi@uohyd.ac.in

Authors

Upasana Phukon − *School of Chemistry, University of Hyderabad, Hyderabad 500 046, India*

Moon Kedia − *School of Chemistry, University of Hyderabad, Hyderabad 500 046, India;* orcid.org/0000-0003-2000-209X

Bhaskaran Shankar − *Department of Chemistry, Thiagarajar College of Engineering, Madurai 625 015, India*

Complete contact information is available at: https://pubs.acs.org/10.1021/acsomega.3c06371

Funding

IoE (UH-IoE-RC3-21−064)

Notes

The authors declare no competing financial interest.

■ ACKNOWLEDGMENTS

The authors thank the University of Hyderabad and IoE for the financial support. U.P. thanks UGC for the fellowship.

■ REFERENCES

(1) Saha, R.; Mondal, B.; Mukherjee, P. S. Molecular Cavity for Catalysis and Formation of Metal Nanoparticles for Use in Catalysis. *Chem. Rev.* **2022**, *122*, 12244−12307.

(2) Samantray, S.; Krishnaswamy, S.; Chand, D. K. Self-Assembled Conjoined-Cages. *Nat. Commun.* **2020**, *11*, No. 880, DOI: 10.1038/s41467-020-14703-4.

(3) Sepehrpour, H.; Fu, W.; Sun, Y.; Stang, P. J. Biomedically Relevant Self-Assembled Metallacycles and Metallacages. *J. Am. Chem. Soc.* **2019**, *141*, 14005−14020.

(4) Pothig, A.; Casini, A. Recent Developments of Supramolecular Metal-based Structures for Applicatins in Cancer Therapy and Imaging. *Theranostics* **2019**, *9*, 3150−3169.

(5) Yu, G.; Jiang, M.; Huang, F.; Chen, X. Supramolecular Coordination Complexes as Diagnostic and Therapeutic Agents. *Curr. Opin. Chem. Biol.* **2021**, *61*, 19−31.

(6) Percástegui, E. G.; Ronson, T. K.; Nitschke, J. R. Design and Applications of Water-Soluble Coordination Cages. *Chem. Rev.* **2020**, *120*, 13480−13544.
(7) Huang, Z.; Wilson, J. J. Therapeutic and Diagnostic Applications of Multimetallic Rhenium(I) Tricarbonyl Complexes. *Eur. J. Inorg. Chem.* **2021**, *2021*, 1312−1324.
(8) Takezawa, H.; Fujita, M. Molecular Confinement Effects by Self-Assembled Coordination Cages. *Bull. Chem. Soc. Jpn.* **2021**, *94*, 2351−2369.
(9) Mishra, I.; Bhol, M.; Kalimuthu, P.; Sathiyendiran, M. Emerging Spacers-Based Ligands for Supramolecular Coordination Complexes. *Chem. Rec.* **2021**, *21*, 594−614.
(10) Dang, L. L.; Feng, H. J.; Lin, Y. J.; Jin, G. X. Self-Assembly of Molecular Figure-Eight Knots Induced by Quadruple Stacking Interactions. *J. Am. Chem. Soc.* **2020**, *142*, 18946−18954.
(11) Forgan, R. S.; Sauvage, J. P.; Stoddart, J. F. Chemical Topology: Complex Molecular Knots, Links, and Entanglements. *Chem. Rev.* **2011**, *111*, 5434−5464.
(12) Ashbridge, Z.; Fielden, S. D. P.; Leigh, D. A.; Pirvu, L.; Schaufelberger, F.; Zhang, L. Knotting Matters: Orderly Molecular Entanglements. *Chem. Soc. Rev.* **2022**, *51*, 7779−7809.
(13) Han, M.; Engelhard, D. M.; Clever, G. H. Self-Assembled Coordination Cages Based on Banana-Shaped Ligands. *Chem. Soc. Rev.* **2014**, *43*, 1848−1860.
(14) Feng, T.; Li, X.; An, Y. Y.; Bai, S.; Sun, L. Y.; Li, Y.; Wang, Y. Y.; Han, Y. F. Backbone-Directed Self-Assembly of Interlocked Molecular Cyclic Metalla[3]Catenanes. *Angew. Chem., Int. Ed.* **2020**, *59*, 13516−13520.
(15) Inomata, Y.; Sawada, T.; Fujita, M. Metal−Peptide Nonafoil Knots and Decafoil Supercoils. *J. Am. Chem. Soc.* **2021**, *143*, 16734−16739.
(16) Cui, Z.; Gao, X.; Lin, Y. J.; Jin, G. X. Stereoselective Self-Assembly of Complex Chiral Radial[5] Catenanes Using Half-Sandwich Rhodium/Iridium Building Blocks. *J. Am. Chem. Soc.* **2022**, *144*, 2379−2386. And References therein.
(17) Cui, Z.; Jin, G. X. Construction of a molecular prime link by interlocking two trefoil knots. *Nat. Synth.* **2022**, *1*, 635−640.
(18) O'Sullivan, M. C.; Sprafke, J. K.; Kondratuk, D. V.; Rinfray, C.; Claridge, T. D. W.; Saywell, A.; Blunt, M. O.; O'Shea, J. N.; Beton, P. H.; Malfois, M.; Anderson, H. L. Vernier Templating and Synthesis of a 12-Porphyrin Nano-Ring. *Nature* **2011**, *469*, 72−75.
(19) Wipf, P.; Fritch, P. C.; Geib, S. J.; Sefler, A. M. Conformational Studies and Structure-Activity Analysis of Lissoclinamide 7 and Related Cyclopeptide Alkaloids. *J. Am. Chem. Soc.* **1998**, *120*, 4105−4112.
(20) West, S. C.; Countryman, J. K.; Howard-Flanders, P. Enzymatic Formation of Biparental Figure-Eight Molecules from Plasmid DNA and Their Resolution in E. coli. *Cell* **1983**, *32*, 817−829.
(21) Huang, J.; Liu, D.; Wang, S.-C.; Chen, M.; Zhao, H.; Li, K.; Chan, Y.-T.; Wang, P. Molecular Lemniscates from Organic-Metal Terpyridine-Based Self-Assembly and Host−Guest Recognition. *Inorg. Chem.* **2019**, *58*, 5051−5057.
(22) Schulte, T. R.; Holstein, J. J.; Schneider, L.; Adam, A.; Haberhauer, G.; Clever, G. H. A New Mechanically-Interlocked $[Pd_2L_4]$ Cage Motif by Dimerization of Two Peptide-based Lemniscates. *Angew. Chem., Int. Ed.* **2020**, *59*, 22489−22493.
(23) Zhang, T. T.; Chen, T.; Dang, L. L.; Li, T. T.; Sun, K. X.; Gao, Y. J.; Ma, L. F.; Li, D. S. Self-Assembly and Near-Infrared Photothermal Conversion Research of Molecular Figure-of-Eight. *J. Solid State Chem.* **2022**, *313*, No. 123320.
(24) Lv, X. P.; Wei, D. H.; Yang, G. Y. Hexameric Silver(I) Pyrazolate: Synthesis, Structure, and Isomerization. *Inorg. Chem.* **2017**, *56*, 11310−11316.
(25) Govindarajan, R.; Divya, D.; Nagarajaprakash, R.; Manimaran, B. Synthesis and Characterization of Aminoquinonato Bridged Re(I)-Based Amide Functionalized Dinuclear Metallastirrups and Tetranuclear Lemniscate Metallacycles. *ChemistrySelect* **2018**, *3*, 3742−3750.
(26) Zhang, Y.; Crawley, M. R.; Hauke, C. R.; Friedman, A. E.; Janik, T. S.; Cook, T. R. A Bis(dipyrrinato) Motif as a Building Block for Polynuclear Rhenium(I) Architectures. *Eur. J. Inorg. Chem.* **2017**, *2017*, 4055−4060.
(27) Dilworth, J. R. Rhenium Chemistry-Then and Now. *Coord. Chem. Rev.* **2021**, *436*, No. 213822.
(28) Bauer, E. B.; Haase, A. A.; Reich, R. M.; Crans, D. C.; Kuhn, F. E. Organometallic and Coordination Rhenium Compounds and Their Potential in Cancer Therapy. *Coord. Chem. Rev.* **2019**, *393*, 79−117.
(29) Schindler, K.; Zobi, F. Anticancer and Antibiotic Rhenium Tri- and Dicarbonyl Complexes: Current Research and Future Perspectives. *Molecules* **2022**, *27*, No. 539, DOI: 10.3390/molecules27020539.
(30) Sharma S, A.; Vaibhavi, N.; Kar, B.; Das, U.; Paira, P. Target-Specific Mononuclear and Binuclear Rhenium(I) Tricarbonyl Complexes as Upcoming Anticancer Drugs. *RSC Adv.* **2022**, *12*, 20264−20295.
(31) Thanasekaran, P.; Lee, C.-C.; Lu, K.-L. One-Step Orthogonal-Bonding Approach to the Self-Assembly of Neutral Rhenium-Based Metallacycles: Synthesis, Structures, Photophysics, and Sensing Applications. *Acc. Chem. Res.* **2012**, *45*, 1403−1418.
(32) Tzeng, B.; Chao, A.; Lin, M.; Lee, G.; Kuo, T. Molecular ReI cages: structural and luminescent properties. *Chem. - Eur. J.* **2017**, *23*, 18033−18040, DOI: 10.1002/chem.201704122.
(33) Procopio, E. Q.; Dova, D.; Cauteruccio, S.; Forni, A.; Licandro, E.; Panigati, M. Dirhenium coordination complex endowed with an intrinsically chiral helical-shaped diphosphine oxide. *ACS Omega* **2018**, *3*, 11649−11654.
(34) Boulay, A.; Seridi, A.; Zedde, C.; Laderia, S.; Picard, C.; Maron, L.; Benoist, E. Tricarbonyl ReI complexes from functionalised pyridine−triazole derivatives: from mononuclear to unexpected dimeric complexes. *Eur. J. Inorg. Chem.* **2010**, 5058−5062, DOI: 10.1002/ejic.201000891.
(35) Sathiyendiran, M.; Tsai, C.; Thanasekaran, P.; Luo, T.; Yang, C.; Lee, G.; Peng, S.; Lu, K. Organometallic calixarenes: syceelike tetrarhenium(I) cavitands with tunable size, color, functionality, and coin−slot complexation. *Chem. - Eur. J.* **2011**, *1*, 3343−3346, DOI: 10.1002/chem.201003181.
(36) Jin, G.-X.; Wang, T.; Sun, Y.; Li, Y.; Ma, J. Photochromic rhenium-based molecular rectangles: syntheses, structures, photophysical properties, and electrochemistry. *Inorg. Chem.* **2020**, *59*, 15019−15027.
(37) Chan, C. Y.; Pellegrini, P. A.; Greguric, I.; Barnard, P. J. Rhenium and technetium tricarbonyl complexes of N-heterocyclic carbene ligands. *Inorg. Chem.* **2014**, *53*, 10862−10873.
(38) Sato, S.; Ishitani, O. Photochemical reactions of fac-rhenium(I) tricarbonyl complexes and their application for synthesis. *Coord. Chem. Rev.* **2015**, *282*−*283*, 50−59.
(39) Sinha, D.; Parua, S. P.; Rajak, K. K. Synthesis and characterization of acrylate cyanide bridged dimeric fac-Rhenium(I) complex: Photophysical, selective CO_2 adsorption and theoretical studies. *J. Organomet. Chem.* **2019**, *889*, 62−69.
(40) Gupta, D.; Sathiyendiran, M. Rhenium-Carbonyl-Based Supramolecular Coordination Complexes: Synthesis, Structure and Properties. *ChemistrySelect* **2018**, *3*, 7439−7458.
(41) Soumya, K. R.; Arumugam, R.; Shankar, B.; Sathiyendiran, M. Sulfate donor based dinuclear heteroleptic triple-stranded helicates from sulfite and ditopic nitrogen donor ligands and their transformation to dinuclear homoleptic double-stranded mesocates. *Inorg. Chem.* **2018**, *57*, 10718−10725.
(42) Arumugam, R.; Shankar, B.; Soumya, K. R.; Sathiyendiran, M. fac-Re(CO)3-based neutral heteroleptic tetrahedrons. *Dalton Trans.* **2019**, *48*, 7425−7431.
(43) Shankar, B.; Marimuthu, R.; Sathiyashivan, S. D.; Sathiyendiran, M. Spheroid metallacycles and metallocavitands with calixarene- and/or cleft-shaped receptors on the surface. *Inorg. Chem.* **2016**, *55*, 4537−4544.
(44) Govindarajan, R.; Nagarajaprakash, R.; Veena, V.; Sakthivel, N.; Manimaran, B. One-pot reaction of amide functionalized Re(I) based dinuclear metallacycles: Synthesis, characterization and evaluation for anticancer potential. *Polyhedron* **2018**, *139*, 229−236.

https://doi.org/10.1021/acsomega.3c06371
ACS Omega 2023, 8, 41773−41784

(45) Huang, G. G.; Lee, C.; Yang, J.; Lu, Z.; Sathiyendiran, M.; Huang, C.; Kao, Y.; Lee, G.; Lu, K. Cavity-containing rhenium metallacycle treated evanescent wave infrared chemical sensors for the selective determination of odorous amines in the atmosphere. *Sens. Actuators, B* **2018**, *254*, 424−430.
(46) Phukon, U.; Shankar, B.; Sathiyendiran, M. Self-assembly of a new class of rhenium(I)-based double stranded dinuclear monohelicates with their photophysical and electrochemical studies. *Dalton Trans.* **2022**, *51*, 16307−16315.
(47) Bhol, M.; Shankar, B.; Sathiyendiran, M. Rhenium(I) based irregular pentagonal-shaped metallacavitands. *Dalton Trans.* **2018**, *47*, 4494−4500.
(48) Kedia, M.; Shankar, B.; Sathiyendiran, M. Rhenium(I)-Based Neutral Coordination Cages with a Spherical Cavity for Selective Recognition of Fluoride. *Inorg. Chem.* **2022**, *61*, 14506−14510.
(49) Bhol, M.; Shankar, B.; Sathiyendiran, M. Rhenium(I)-Based Heteroleptic Pentagonal Toroid-Shaped Metallocavitands: Self-Assembly and Molecular Recognition Studies. *Inorg. Chem.* **2022**, *61*, 11497−11508.
(50) Bhol, M.; Claude, G.; Jungfer, M. R.; Abram, U.; Sathiyendiran, M. Calix[4]arene-Analogous Technetium Supramolecules. *Inorg. Chem.* **2022**, *61*, 5173−5177, DOI: 10.1021/acs.inorgchem.1c03691.
(51) Shankar, B.; Marimuthu, R.; Sathiyashivan, S. D.; Sathiyendiran, M. Spheroid Metallacycles and Metallocavitands with Calixarene- and/or Cleft-Shaped Receptors on the Surface. *Inorg. Chem.* **2016**, *55*, 4537−4544.
(52) Lin, S. M.; Velayudham, M.; Tsai, C. H.; Chang, C. H.; Lee, C. C.; Luo, T. T.; Thanasekaran, P.; Lu, K. L. A Molecular Triangle as a Precursor Toward the Assembly of a Jar-Shaped Metallasupramolecule. *Organometallics* **2014**, *33*, 40−44.
(53) Kedia, M.; Priyatharsini, M.; Sathiyashivan, S. D.; Shankar, B.; Krishnakumar, R. V.; Sathiyendiran, M. Prototype Rhenium Metallocavitand with Four Exocyclic Cavities for Small Molecules. *J. Organomet. Chem.* **2022**, *959*, 122123−122129.
(54) Phukon, U.; Priyatharsini; Sathiyendiran, M. Self-assembly of rhenium core-based conjoined bicyclic supramolecule from pyrazole and flexible hexatopic pyrazolyl ligands. *J. Organomet. Chem.* **2020**, *923*, No. 121460.
(55) Sathiyendiran, M.; Tsai, C.-C.; Thanasekaran, P.; Luo, T.-T.; Yang, C.-I.; Lee, G.-H.; Peng, S.-M.; Lu, K.-L. Organometallic Calixarenes: Syceelike Tetrarhenium(I) Cavitands withTunable Size, Color, Functionality, and Coin−Slot Complexation. *Chem. - Eur. J.* **2011**, *17*, 3343−3346, DOI: 10.1002/chem.201003181.
(56) Dinolfo, P. H.; Williams, M. E.; Stern, C. L.; Hupp, J. T. Rhenium-Based Molecular Rectangles as Frameworks for Ligand-Centered Mixed Valency and Optical Electron Transfer. *J. Am. Chem. Soc.* **2004**, *126*, 12989−13001.
(57) Bhattacharya, D.; Sathiyendiran, M.; Luo, T.-T.; Chang, C.-H.; Cheng, Y.-H.; Lin, C.-Y.; Lee, G.-H.; Peng, S.-M.; Lu, K.-L. Ground and Excited Electronic States of Quininone-Containing Re(I)-Based Rectangles: a Comprehensive Study of Their Preparation, Electrochemistry, and Photophysics. *Inorg. Chem.* **2009**, *48*, 3731−3742.
(58) Xiong, J.; Liu, W.; Wang, Y.; Cui, L.; Li, Y.-Z.; Zuo, J.-L. Tricarbonyl Mono- and Dinuclear Rhenium(I) Complexes with RedoxActive Bis(pyrazole)−Tetrathiafulvalene Ligands: Syntheses, Crystal, Structures, and Properties. *Organometallics* **2012**, *31*, 3938−3946.
(59) Ning, G. H.; Yao, L. Y.; Liu, L. X.; Xie, T. Z.; Li, Y. Z.; Qin, Y.; Pan, Y. J.; Yu, S. Y. Self-assembly and host-guest interaction of metallomacrocycles using fluorescent dipyrazole linker with dimetallic clips. *Inorg. Chem.* **2010**, *49*, 7783−7792.
(60) Desiraju, G. R. Hydrogen bonds and other intermolecular interactions in organometallic crystals. *J. Chem. Soc., Dalton Trans.* **2000**, 3745−3751.
(61) Merillas, B.; Cuéllar, E.; Diez-Varga, A.; Torroba, T.; García-Herbosa, G.; Fernández, S.; Lloret-Fillol, J.; Martín-Alvarez, J. M.; Miguel, D.; Villafañe, F. Luminescent Rhenium(I) tricarbonyl Complexes Containing Different Pyrazoles and Their Successive Deprotonation Products: CO_2 Reduction Electrocatalysts. *Inorg. Chem.* **2020**, *59*, 11152−11165.
(62) Horiuchi, S.; Umakoshi, K. Recent advances in pyrazolato-bridged homo- and heterometallic polynuclear platinum and palladium complexes. *Coord. Chem. Rev.* **2023**, *476*, No. 214924.
(63) Guerrero, M.; Pons, J.; Brabcgadell, V.; Parella, T.; Solans, X.; Font-Bardia, M.; Ros, J. Synthesis and characterization of metallomacrocyclic palladium(II) complexes with new hybrid pyrazole ligands. Diffusion NMR studies and theoretical calculations. *Inorg. Chem.* **2008**, *47*, 11084−11094.
(64) Samanta, D.; Mukherjee, P. S. Component Selection in the Self-Assembly of Palladium(II) Nanocages and Cage-to-Cage Transformations. *Chem. - Eur. J.* **2014**, *20*, 12483−12492, DOI: 10.1002/chem.201402553.
(65) Ghosh, S.; Mukherjee, P. S. Self-Assembly of Metallamacrocycles via a Rigid Phosphorous Donor Linker. *Organometallics* **2007**, *26*, 3362−3367.
(66) Wang, W.; Wang, Y. X.; Yang, H. B. Supramolecular transformations within discrete coordination-driven supramolecular architectures. *Chem. Soc. Rev.* **2016**, *45*, 2656−2693.
(67) Benchimol, E.; Nguyen, B. N. T.; Ronson, T. K.; Nitschke, J. R. Transformation networks of metal−organic cages controlled by chemical stimuli. *Chem. Soc. Rev.* **2022**, *51*, 5101−5135.
(68) Garci, A.; Marti, S.; Schurch, S.; Therrien, B. Insight into the dynamic ligand exchange process involved in bipyridyl linked arene ruthenium metalla-rectangles. *RSC Adv.* **2014**, *4*, 8597−8604.
(69) Bravo, J.; Bolaño, S.; Gonsalvi, L.; Peruzzini, M. Coordination chemistry of 1,3,5-triaza-7-phosphaadamantane (PTA) and derivatives. Part II. The quest for tailored ligands, complexes and related applications. *Coord. Chem. Rev.* **2010**, *254*, 555−607.
(70) Chakraborty, I.; Carrington, S. J.; Roseman, G.; Mascharak, P. K. Synthesis, Structures, and CO Release Capacity of a Family of Water Soluble PhotoCORMs: Assessment of the Biocompatibility and Their Phototoxicity toward Human Breast Cancer Cells. *Inorg. Chem.* **2017**, *56*, 1534−1545.
(71) Alguacil, A.; Scalambra, F.; Romerosa, A. Insights into the κ-P,N Coordination of 1,3,5-Triaza-7-phosphaadamantane and Derivatives: κ-P,N-Heterometallic Complexes and a 15N Nuclear Magnetic Resonance Survey. *Inorg. Chem.* **2022**, *61*, 5779−5791, DOI: 10.1021/acs.inorgchem.1c03831.
(72) Sheldrick, G. M. A short history of SHELX. *Acta Crystallogr., Sect. A: Found. Crystallogr.* **2008**, *64*, 112−122.
(73) Sheldrick, G. M. *SHELXS-97: Program for Crystal Structure Solution*; University of Göttingen: Göttingen, Germany, 1997.

https://doi.org/10.1021/acsomega.3c06371
ACS Omega 2023, 8, 41773−41784